Chapter 4: Results – presentation and discussion

In chapter 3 I discussed the design and methodology of the test program in more detail. In chapter 4 the results from this test program are presented and discussed. The discussion is broken down into four parts. In all four parts the results are represented and discussed in one paragraph and the concluding remarks made in another. The four parts are:

4.1 Characterise crude ilmenite, LSR, chromite in LSR and UG 1 chromite before roasting
4.2 Characterise crude ilmenite, LSR, chromite in LSR and UG 1 chromite after roasting
4.3 Fractionate crude ilmenite, LSR and UG 1 chromite before roasting
4.4 Fractionate crude ilmenite, LSR and UG 1 chromite before roasting

4.1 Characterize crude ilmenite, LSR, chromite in LSR and UG 1 chromite before roasting

4.1.1 Presentation and discussion of results

4.1.1.1 Chemical analyses

The average chemical compositions of the unroasted crude ilmenite, LSR[11], chromite in LSR and UG1 chromite are presented in table 4.1. During sample preparation thirty-two per cent of the crude ilmenite feed sample reported as LSR. When comparing the chemical analyses in table 4.1 with the mineralogical analyses in table 4.3 one notices that even though one third of the ilmenite and the majority of the rutile from the crude ilmenite reported in the LSR (table 4.3), the TiO_2 content of LSR at 39 per cent was significantly lower than that of crude ilmenite at 45 per cent (table 4.1 for the optimization material). This could be attributed to the high concentration of other non-magnetic material in the LSR (table 4.3). Hammerbeck (1976) published the TiO_2 content of ilmenite in KwaZulu-Natal, South Africa, as 49.0-49.7 per cent.

Table 4.1: Chemical composition, in mass per cent, of the unroasted crude ilmenite and the LSR (XRF results), the chromite in the LSR with a) the EDX results and b) the WDS results and the unroasted UG 1 chromite WDS results.

Sample	TiO_2	Fe_{tot}	FeO	Fe_2O_3	MgO	Al_2O_3	CaO	V_2O_5	Cr_2O_3	MnO	SiO_2	K_2O	P_2O_5	ZrO_2	Fe^{2+}	Fe^{3+}
Crude [12]	45.3	-	-	-	0.6	0.7	0.3	0.3	0.2	1.1	3.4	0.0	0.1	0.9	25.7	9.8
LSR[13]	39.2	-	-	-	0.7	1.6	0.7	0.2	0.6	1.1	7.8	0.1	0.3	3.2	25.7	17.1
Crude [14]	47.1	36.8	-	-	0.4	0.3	0.0	0.3	0.2	1.1	0.3	ND	0.0	0.1	-	-
LSR[15]	41.5	38.7	-	-	0.4	0.7	0.0	0.2	0.6	1.1	1.2	0.0	0.1	0.4	-	-
Chromite in LSR[a]	-	-	25	4	7	22	-	-	42	-	-	-	-	-	-	-
Chromite in LSR[b]	-	-	26	12	6	17	-	-	39	-	-	-	-	-	-	-
UG 1 Chromite	-	-	19	12	10	16	-	-	43	-	-	-	-	-	-	-

The Cr_2O_3 content of the crude ilmenite sample in table 4.1 is 0.21 per cent, far less than the typical value of 0.3 per cent published by Nell and Den Hoed (1997). At 0.56 per cent the Cr_2O_3 content of LSR was high.

Two types of behaviour were observed when analyzing the other components (table 4.1):

- The concentration of the component remained relatively constant when comparing the LSR with crude ilmenite; or
- The component was concentrated in the LSR fraction when comparing the LSR with crude ilmenite.

[11] Low susceptibility rejects
[12] Optimisation tests
[13] Optimisation tests
[14] Fractionation tests
[15] Fractionation tests

MgO, MnO and V_2O_5 were components that followed the first behaviour pattern. One explanation for this was that these components were in solid solution in ilmenite, as stated by Nell and Den Hoed (1997). CaO, SiO_2 and Al_2O_3 were examples of components that followed the second behaviour pattern. These components were part of discrete particles with low magnetic susceptibility. The CaO content of the LSR was 2.1 times more than that of crude ilmenite. This can only be attributed to contamination of the sample by Ca-containing material, such as cement, during preparation of the LSR sample. Both the ZrO_2 and the P_2O_5 levels were more than 3 times higher than that of the crude ilmenite. The discrepancy on the P_2O_5 was attributed to the very low P_2O_5 content of the mineral leading to inaccurate determination of the P_2O_5 content by XRF. The difference in ZrO_2 analysis was due to the concentration of zircon in the LSR – refer to table 4.3. For the purpose of the study the K_2O content of both streams was negligible.

As stated in chapter 2 all natural magnesiochromites contain a considerable amount of Fe^{2+} (which replaces Mg^{2+}) and Al^{3+} or Fe^{3+} (replacing Cr^{3+}). In natural chromites a considerable amount of Mg^{2+} replaces Fe^{2+} with generally appreciable replacement of Cr^{3+} by Al^{3+}, but less so by Fe^{3+} (Deer et al 1966). Both the EDX and the WDS results in table 4.1 confirmed that the chromite in the LSR was of the magnesiochromite spinel series. From table 4.1 the chromite in the LSR contained a considerable amount of MgO. The results of the two analysis methods – EDX and WDS – can be seen to be similar.

The distribution of iron between the divalent and trivalent states was estimated, based on the assumption that all the chromium is trivalent and that the spinel is stoichiometric M_3O_4. The procedure for this estimation is given in Appendix 2 at the end of this chapter.

The results in table 4.1 indicate that the chromite in the UG1 sample was not only of the magnesiochromite spinel series, but also very close in composition to that of the chromite in the LSR with slightly less Al_2O_3 and more Cr_2O_3. However, the match was not perfect, since the average Fe_2O_3: FeO mass ratio of the chromite in the LSR was 0.50 whereas that of the chromite in the UG1 sample 0.64. It was therefore expected that oxidising roasting would have a greater effect on the magnetic susceptibility of the chromite in the LSR than the chromite in the UG1 sample (since trivalent iron enhances the magnetic susceptibility of chromite).

4.1.1.2 Mineralogical analyses

From the XRD results in table 4.2 both crude ilmenite and the LSR consisted of ilmenite and hematite, but the *quantities* of the minerals could not be identified with this method. As the diffraction patterns for pseudobrookite, rutile and quartz were not clear this method was also inefficient in determining the *differences* between the various fractions.

Table 4.2: Phase-chemical composition of crude ilmenite and LSR (XRD results).

Description	Main phases	Minor phases	Trace phases
Crude	Ilmenite	-	Hematite, (Pseudobrookite?)
LSR	Ilmenite	-	Hematite, (Rutile?)

Legend: *Ilmenite – $FeTiO_3$; Hematite – Fe_2O_3; Pseudobrookite – Fe_2TiO_5; Quartz – SiO_2; Rutile – TiO_2.*

The results of a QEMSEM investigation in table 4.3 confirmed the XRD results as all fractions consisted of ilmenite and iron bearing minerals. *Crude ilmenite* contained 90.8 per cent ilmenite, 2.3 per cent other valuable heavy minerals (zircon and rutile), 0.4 per cent chromite and equal amounts (3.3 per cent) of iron oxides and other gangue minerals (primarily SiO_2 bearing). Zircon and rutile reported in the crude ilmenite due to inefficient separation in the WHIMS. The *LSR fraction* had high iron oxide (3.9 per cent), chromite (1.1 per cent), valuable heavy mineral (6.1 per cent) and gangue mineral (4.2 per cent) contents and had low ilmenite content (84.6 per cent). In table 4.3 ninety percent of the valuable heavy minerals (VHM) and chromite, two thirds of the iron oxide and other gangue minerals, and a third of the ilmenite concentrated in the LSR fraction. From these results it was clear that the LSR fraction contained the majority of the unwanted minerals contained in crude ilmenite.

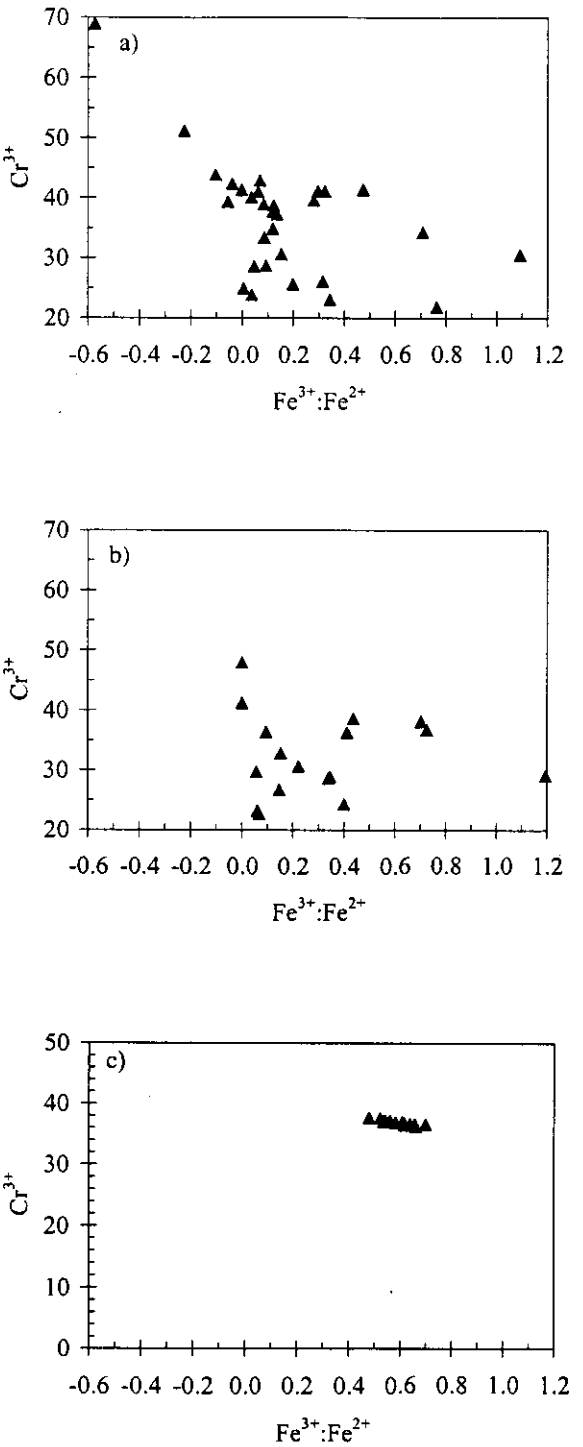

Figure 4.1: The variation in chemical analysis of the chromite in unroasted LSR, indicated by the normalized mole percentage Cr^{3+} and the $Fe^{3+}:Fe^{2+}$ ratio of the calculated mole percentage Fe^{3+} and Fe^{2+}, based on a) the EDX analysis of 30 particles and b) the WDS analysis of 18 particles. c) Results for unroasted UG1 chromite (showing the WDS analysis of 15 particles).

Table 4.3: Modal analysis of the crude ilmenite and LSR (reported in mass per cent).

Phase	Crude	LSR	Phase	Crude	LSR
Ilmenite	90.8	84.6	Siliceous Leucoxene	0.6	0.8
Fe-oxide	3.3	3.9	Quartz	0.9	0.6
Chromite	0.4	1.1	Other silicates	1.6	2.1
Zircon	1.5	4.7	Monazite	0.1	0.5
Rutile	0.8	1.4	Sulphide	0.1	0.2
Total				100	100

The results of the QEMSEM analysis in table 4.4 present the results in table 4.3 in more detail. Crude ilmenite contained more unaltered ilmenite (66.0 per cent) than LSR (44.0 per cent). LSR contained more altered ilmenite (24.1 per cent) than crude ilmenite (20.2 per cent). The impact of the unaltered and altered ilmenite content on magnetic susceptibility and roasting was not clear. Being the fraction with lower magnetic susceptibility the LSR contained double the amount of hematite, five times as much rutile, 2.5 times as much zircon and monazite, 1.5 times as much chromite and 4 times as much gangue material, when compared to crude ilmenite. These minerals would not be affected by roasting.

Table 4.4: Semi-quantitative phase distribution of the crude ilmenite and LSR (reported in mass per cent).

Particles	Crude	LSR
Homogenous, unaltered ilmenite	66.0	44.0
Slightly altered ilmenite // micro-fractures, grain boundaries, (0001)	12.6	13.2
Moderately altered ilmenite // micro-fractures, grain boundaries, (0001)	1.2	2.0
Alteration involving development of fine rutile lenses & titano-hematite	0.6	0.4
Partial heterogeneous alteration	2.4	2.4
Moderate heterogeneous alteration	0.8	2.3
Extensive heterogeneous alteration	2.6	3.8
Ilmenite with exsolved Hematite	2.2	1.4
Ilmenite-Hematite	0.1	0.3
Hematite with exsolved Ilmenite	0.8	1.0
Titano-hematite	0.4	1.3
Hematite	5.0	9.4
Porous aggregates of TiO_2-crystals & Secondary Rutile/Anatase	0.4	1.0
Primary Rutile	0.3	1.5
Zircon and Monazite	1.8	5.0
Chromite	0.5	1.3
Goethite	0.3	1.8
Gangue	2.0	7.9
Total	100	100

From table 4.5 the Fe-oxide grains contained small inclusions of rutile and/or silicate minerals. For classifications purposes grains containing more than 80 per cent Fe-oxide were considered liberated. The data showed that about one third of the Fe-oxide grains in the crude ilmenite were liberated. The composite Fe-oxide-silicate grains were predominant in the LSR. Complex intergrowths of rutile, quartz and/or other silicates, ilmenite and hematite were present in both the crude ilmenite and the LSR.

Table 4.5: Occurrence of Fe-oxide (reported as percent by volume).

	Crude	LSR
Total no. grains analyzed	>1000	>1000
No. Fe-oxide bearing grains	53	87
Volume percent Fe-oxides in Fe-oxide bearing grains		
>80% Fe-oxides (liberated)	33	28
60%<Fe-oxides<80%	21	35
40%<Fe-oxides<60%	21	7
20%<Fe-oxides<40%	15	11
<20% Fe-oxides	10	9
Phase associations[16] of composite grains (<80% Fe-oxides)		
Fe-oxide associations	**Crude**	**LSF**
Ilmenite	7	9
Silicates	13	25
Ternary/Composite	47	38

4.1.1.3 Magnetic susceptibility

Table 4.6 reports the magnetic susceptibility of unroasted crude ilmenite, LSR and UG1 chromite.

Table 4.6: Measured magnetic susceptibility of unroasted crude ilmenite, LSR and UG 1 chromite and the magnetic susceptibility of the low susceptibility and high susceptibility peaks of the bimodal Cr_2O_3 peaks and the TiO_2 peak of unroasted crude ilmenite reported by Nell and Den Hoed (1997) reported in cgs units as $*10^{-6}$ cm^3/g.

Sample	Magnetic susceptibility
Unroasted crude ilmenite	188
Unroasted LSR	113
Unroasted UG 1 chromite	149
Low susceptibility peak of the bimodal Cr_2O_3 peaks of unroasted crude ilmenite	20 (range was 20-65)
TiO_2 peak of unroasted crude ilmenite	100 (range was 65-500)
High susceptibility peak of the bimodal Cr_2O_3 peaks of unroasted crude ilmenite	1995 (range was 500-10000)

4.1.1.4 Size analyses

The typical size analysis of the crude ilmenite and for the LSR was a d_{50} of 140μm with fifty percent of the particles in the range 125-180μm and only 1.8 per cent below 75μm. The UG 1 chromite had a d_{50} of 90μm.

4.1.2 Concluding interpretation

4.1.2.1 Chemical analysis

The TiO_2 content of both crude ilmenite and LSR was significantly less than that published by Hammerbeck (1976). This decrease was attributed to the presence of other minerals in both concentrate streams.

It was expected that due to its low Cr_2O_3 content the maximum requirement of 0.1 per cent Cr_2O_3 would easily be met when beneficiating the crude ilmenite by roasting and magnetic separation. On the

[16] Phase association data refer to composite grains (<80 per cent Fe-oxides present). For example, 33 per cent of the Fe-oxide in the crude ilmenite occurred as liberated grains. Of the remaining 67 per cent Fe-oxide in this sample 7 per cent occurred in particles consisting only of Fe-oxide and ilmenite, 13 per cent occurs in particles consisting only of Fe-oxide and silicates and 47 per cent occurs in complex grains.

other hand meeting the maximum requirement of 0.1 per cent Cr_2O_3 when beneficiating LSR would only be possible if roasting:

- Increased the magnetic properties of the ilmenite in the LSR dramatically;
- Did not increase the magnetic properties of Cr_2O_3 at all; and
- If Cr_2O_3 were only present in the LSR fraction as discrete non-ilmenite particles.

If one assumed that the titration results were an indication of what the ilmenite mineral composition was, the magnetic susceptibility of both the crude ilmenite and LSR would be enhanced by oxidative roasting. This is based on the assumption that in ilmenite the maximum magnetic enhancement is achieved when the mole ratio Fe_2O_3:FeO is within the range 1:1 - 1.57:1 (Walpole 1991). The Fe_2O_3:FeO ratio of crude ilmenite was 0.44 and that of LSR 0.78. Oxidation would increase the Fe_2O_3 content of the ilmenite and decrease the FeO content, as per reaction 4.1, and therefore the Fe_2O_3:FeO ratio.

$$FeO + \tfrac{1}{2}O_2 = \tfrac{1}{2}Fe_2O_3$$

Reaction 4.1: Oxidation reaction taking place during the oxidation of ilmenite

No amount of roasting and/or magnetic separation would decrease the content of MgO, MnO and V_2O_5 in the final ilmenite product, because these components are in solid solution in the ilmenite.

If only the magnetic susceptibility of the ilmenite in crude ilmenite or LSR was increased, the content of CaO, SiO_2 and Al_2O_3 in the final ilmenite product could be decreased by magnetic separation.

Despite the lower FeO: Fe_2O_3 mass in the UG 1 chromite, this natural chromite was considered to be sufficiently close in composition to that in the LSR to provide a test of the hypothesis that oxidising roasting leaves the magnetic susceptibility of the chromite unchanged.

4.1.2.2 Mineralogical analysis

XRD was not a very useful method for mineralogical analysis of the crude ilmenite nor that of the LSR. From the other mineralogical analysis methods in the order of 30 per cent of the ilmenite in crude ilmenite reported to LSR. Of this 65 per cent were unaltered ilmenite and 35 per cent altered ilmenite vs. 75 per cent unaltered ilmenite and 25 per cent altered ilmenite in crude ilmenite. When preparing LSR from crude ilmenite the majority of the iron oxides, chromite, other valuable heavy minerals and gangue minerals reported in the LSR.

4.1.2.3 Magnetic susceptibility

As expected the magnetic susceptibility of crude ilmenite was higher than that of LSR. The magnetic susceptibility of the LSR was similar to and that of the crude ilmenite 1.8 times that of the peak magnetic susceptibility in the fractionation curve reported by Nell and Den Hoed (1997). The magnetic susceptibility of the UG 1 samples was in between – higher than that of the LSR and lower than that of the crude ilmenite. The magnetic susceptibility of the UG 1 chromite was higher than that of the low susceptibility peak of the bimodal Cr_2O_3 distribution reported by Nell and Den Hoed (1997), but considerably less than that of the high susceptibility peak. This could be attributed to the higher Fe_2O_3: FeO mass ratio in the unroasted UG 1 chromite compared to that of the chromite in the LSR (De Waal and Copelowitz 1972). Typically, the magnetic susceptibility of UG 1 chromite is some 90 x 10^{-6} cm^3/g (De Waal and Copelowitz 1972).

4.1.2.4 Size analyses

As reported from literature (Svoboda 1987) the only forces on a particle in a Frantz isodynamic separator are the applied magnetic field (H) and gravity. From chapter 2 (Svoboda 1987) the gravity force on a particle in a Frantz isodynamic separator is neglible and therefore size distribution could therefore be neglected as part of this study. .

4.2 Characterization of crude ilmenite, LSR, chromite in LSR and UG 1 chromite after roasting

4.2.1 Presentation and discussion of results

To investigate the effect of roasting atmosphere on the magnetic susceptibility, LSR was roasted in air and in 50:50 air-CO_2 gas mixtures. The results are presented in table 4.7 and graphically presented in figure 4.2. The resulting increase in magnetic susceptibility was calculated as per equation 4.1. The results were presented in table 4.7.

$$a = c/b$$

Equation 4.1: Equation to calculate the increase in magnetic susceptibility

Legend for equation 4.1:
a = Relative increase in magnetic susceptibility
b = Magnetic susceptibility of unroasted sample
c = Magnetic susceptibility of sample roasted at specific conditions

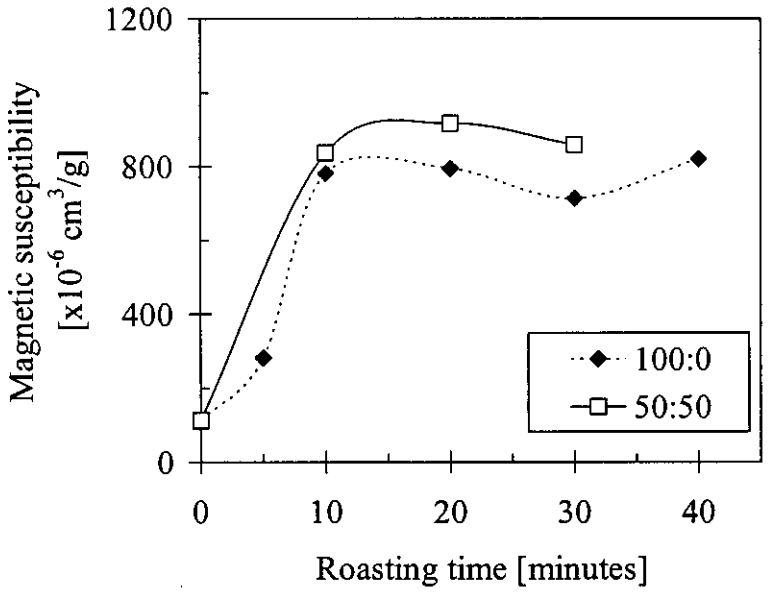

Figure 4.2: Effect of roasting atmosphere on the magnetic susceptibility of LSR.

Table 4.7: The magnetic susceptibility (reported as $*10^{-6}$ cm^3/g) of LSR roasted in air at 750°C in different atmospheres and resulting increase in magnetic susceptibility when roasting LSR at 750°C in different atmospheres

Time [Minutes]	Magnetic susceptibility		Increase in magnetic susceptibility	
	Atmosphere [air: CO_2]		Atmosphere [air: CO_2]	
	100:0	50:50	100:0	50:50
0	113	113	0	0
5	282	-	169	-
10	781	836	668	723
20	794	917	681	804
30	713	858	600	745
40	820	-	707	-

To investigate the effect of roasting temperature on the magnetic susceptibility, LSR was roasted in air at different temperatures. The results are presented in table 2.8 and graphically presented in figure 4.3. The resulting increase in magnetic susceptibility was also calculated with equation 1. The results are presented in table 4.8.

Table 4.8: The magnetic susceptibility (reported as $*10^{-6}$ cm^3/g) of LSR roasted in air at different temperatures and resulting increase in magnetic susceptibility when roasting LSR in air at different temperatures

Time [Minutes]	Magnetic susceptibility Temperature [°C]				Increase in magnetic susceptibility Temperature [°C]			
	700	750	8000	850	700	750	800	850
0	113	113	113	113	0	0	0	0
5	310	282	1081	1110	197	169	968	997
10	394	781	1018	440	281	668	905	327
20	415	794	493	215	302	681	380	102
30	602	713	302	139	489	600	189	26
40	454	820	215	99	341	707	102	-14

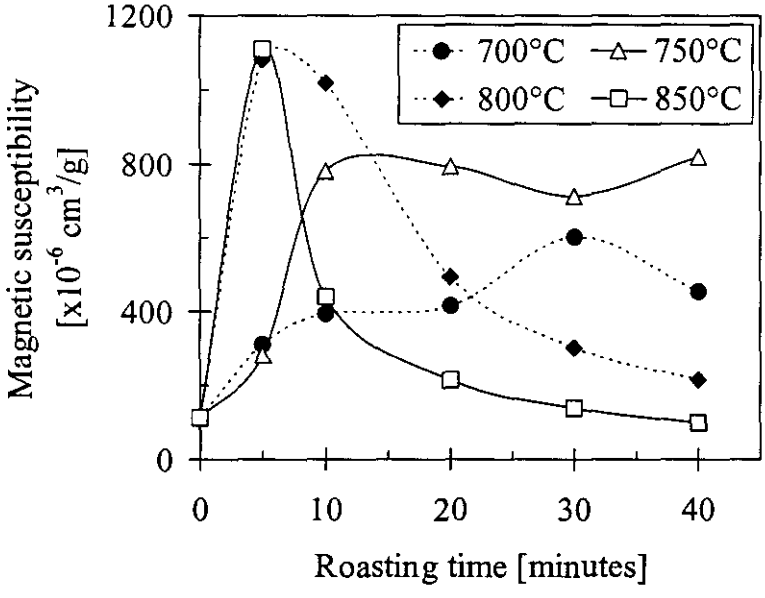

Figure 4.3: Effect of roasting temperature on the magnetic susceptibility of LSR.

From figure 4.2 and figure 4.3 the effect of a factor two change in the oxygen content of the roasting atmosphere on the increase in magnetic susceptibility of LSR was negligible compared to the effect of temperature. Figure 4.3 also indicates that there is no single, ideal set of roasting conditions for LSR. The largest increase in magnetic susceptibility was observed when roasting samples at high temperatures. The magnetic susceptibility increased ten-fold after 5 minutes of roasting at 800°C and 850°C. At 850°C the magnetic susceptibility decreased rapidly with further roasting. At 800°C very good results were obtained after 10 minutes. Even after 20 minutes the benchmark five- to six-fold increase, used by Nell and Den Hoed (1997), was still reached. Longer reaction times resulted in unacceptably low magnetic susceptibility values. Nell and Den Hoed (1997) also observed this phenomenon and stated that it was due to excessive Fe^{3+} formation with the formation of small amounts of pseudobrookite in the most oxidised samples.

Samples of crude ilmenite were also roasted to confirm the roasting conditions determined by Nell and Den Hoed (1997) and to compare the roasting behaviour of LSR with that of the crude ilmenite from which it was beneficiated. The results are presented in table 2.9 and graphically presented in figure 4.4. The resulting increase in magnetic susceptibility was also calculated with equation 4.1. The results were presented in table 2.9.

Table 4.9: The magnetic susceptibility (reported as $*10^{-6}$ cm^3/g) of LSR and crude ilmenite roasted in air at different temperatures and resulting increase in magnetic susceptibility when roasting LSR and crude ilmenite in air at different temperatures

Time [Minutes]	Magnetic susceptibility				Increase in magnetic susceptibility			
	Temperature [°C]				Temperature [°C]			
	750		800		750		800	
	Crude ilmenite	LSR	Crude ilmenite	LSR	Crude ilmenite	LSR	Crude ilmenite	LSR
0	188	113	188	113	0	0	0	0
5	1149	282	1168	1081	961	169	980	968
10	1159	781	847	1018	971	668	659	905
20	1022	794	401	493	834	681	213	380
30	1039	713	259	302	851	600	71	189
40	929	820	182	215	741	707	-6	102

In figure 4.5 the effect of temperature on the magnetic susceptibility of crude ilmenite and that of LSR is compared. At 750°C crude ilmenite had a 12-75 per cent higher increase in magnetic susceptibility compared to LSR. At 800°C the increases in susceptibility for crude ilmenite and LSR were similar, but with differences in rate.

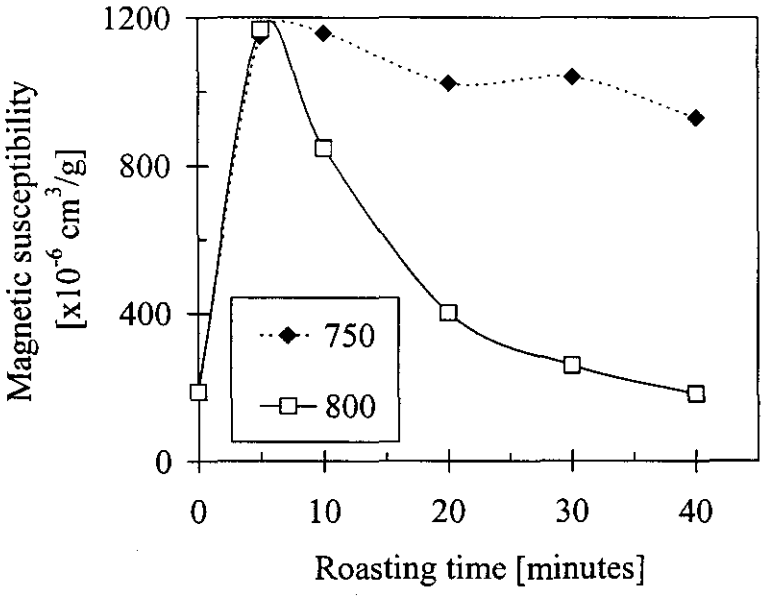

Figure 4.4: Effect of roasting temperature (in °C) on the magnetic susceptibility of crude ilmenite.

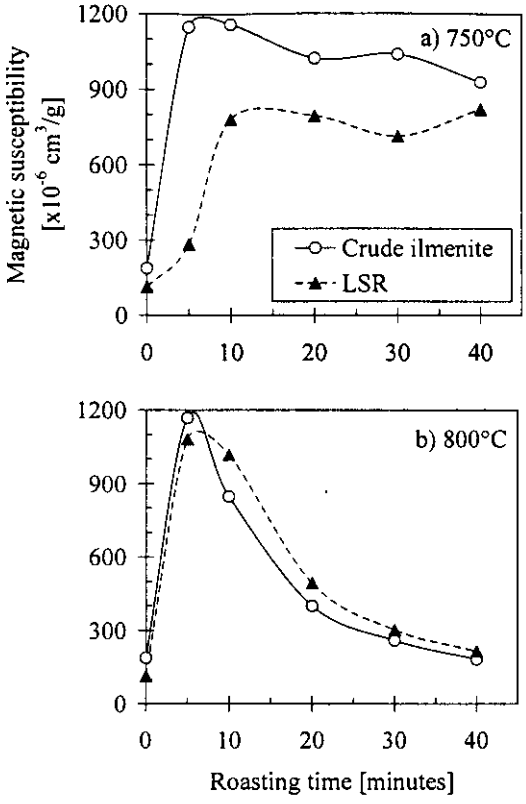

Figure 4.5: The effect of roasting temperature on the magnetic susceptibility of LSR vs. that of crude ilmenite.

The effect of oxidizing roasting at different temperatures and for different time intervals, on the magnetic susceptibility of the UG1 chromite samples, is summarized in Table 4.10. The results in Table 4.10 are plotted in Figure 4.6. The results in Figure 4.6 illustrate that oxidizing roasting did indeed affect the (average) magnetic susceptibility of the UG1 chromite. At all the roasting conditions evaluated the magnetic susceptibility of the roasted samples increased, by factors ranging from 1.4 to 2.6.

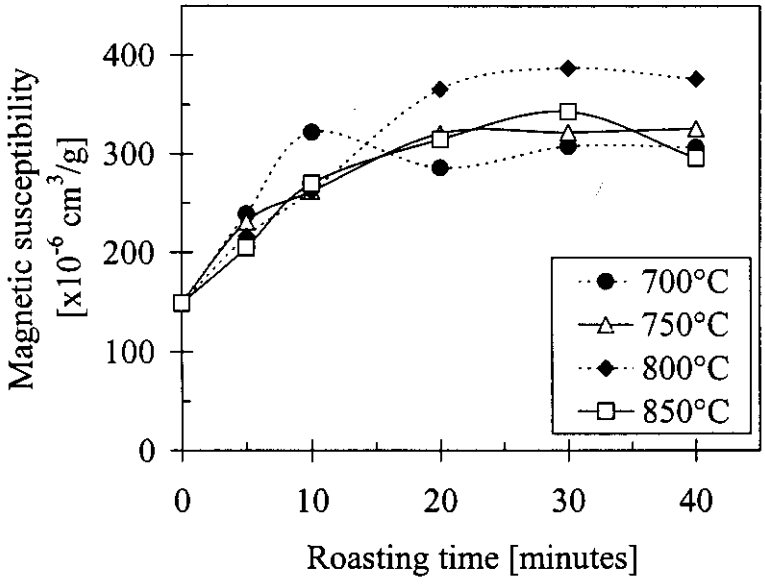

Figure 4.6: Effect of roasting temperature on the magnetic susceptibility of UG1 chromite.

Table 4.10: The magnetic susceptibility (reported as $*10^{-6}$ cm^3/g) of UG 1 chromite roasted in air at different temperatures and resulting increase in magnetic susceptibility when roasting UG 1 chromite in air at different temperatures

Time [Minutes]	Magnetic susceptibility				Increase in magnetic susceptibility			
	Temperature [°C]				Temperature [°C]			
	700	750	800	850	700	750	800	850
0	149	149	149	149	0	0	0	0
5	239	231	216	205	90	82	67	56
10	322	262	262	270	173	113	113	121
20	286	321	366	315	137	172	217	166
30	308	322	387	343	159	173	238	194
40	307	326	376	296	158	177	227	147

From table 4.11 the composition of the unroasted and the roasted UG 1 chromite virtually remained the same only with a slight increase in the Fe_2O_3 content..

Table 4.11: Average chemical composition (WDS), in mass per cent, of the UG 1 chromite roasted at 750°C for 20 minutes in air as well as unroasted UG 1 chromite.

Sample	Number of particles analysed	FeO	Fe_2O_3	MgO	Al_2O_3	Cr_2O_3
UG 1 chromite roasted in fluidised bed roaster	16	22	8	8	16	46
UG 1 chromite roasted in Linn furnace	16	22	9	8	16	45
Unroasted UG 1 chromite	15	19	12	10	16	43

In figure 4.7a) and figure 4.7b) the lack of variation in chemical composition of unroasted and roasted UG1 chromite is illustrated.

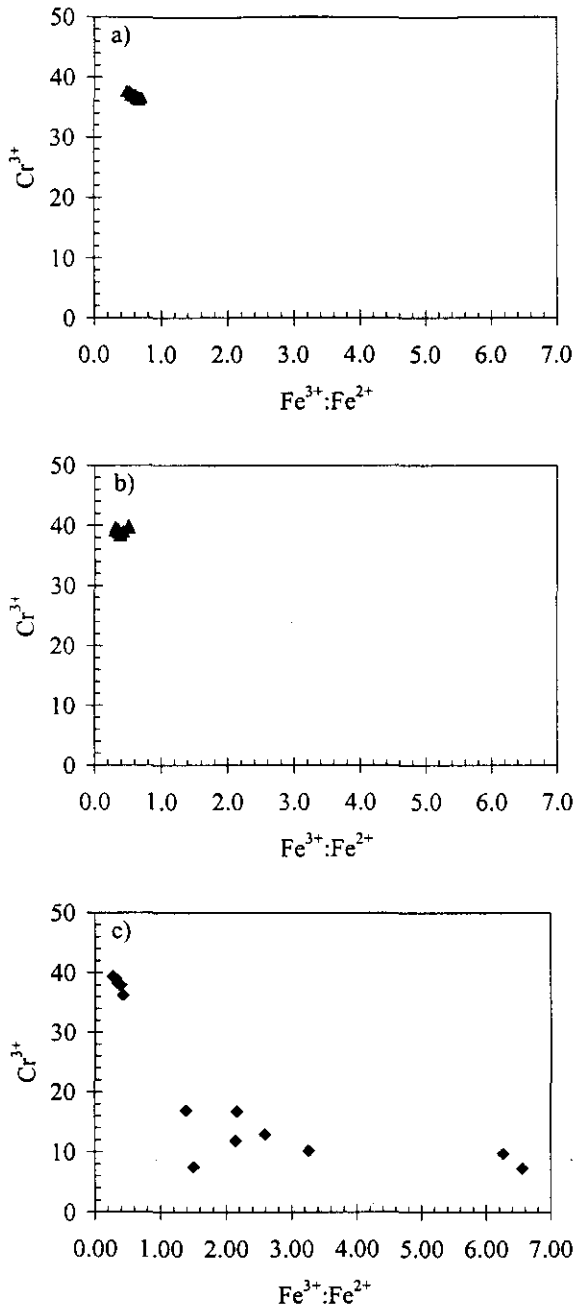

Figure 4.7: The variation in chemical analysis of the UG1 chromite, indicated by the normalized mole percentage Cr^{3+} and the $Fe^{3+}:Fe^{2+}$ ratio of the calculated mole percentage Fe^{3+} and Fe^{2+}, based on a) the WDS analysis of 15 unroasted particles and b) the WDS analysis of 16 particles roasted at 750°C in air for 20 minutes. c) Results for the iron rich layer as well as the chromite rich matrix of the roasted UG1 chromite (showing the EDX analysis of 16 points).

The roasting conditions used in this test program do not seem to oxidize the Fe^{2+} in the chromite as in the ilmenite. If this is the case then the increase in the magnetic susceptibility of the chromite observed in figure 4.6 is due to a mechanism other than a change in the solid solution composition of the chromite caused by reaction 1. The behaviour (increase in magnetic susceptibility after roasting) is the opposite of that observed by Schwerer and Gundaker (1975). The surface structure observed by Schwerer and Gundaker (1975) displayed ferromagnetic behaviour and was *recovered* during annealing i.e. might well have been surface defect structures. EDX analysis of different areas of roasted UG1 chromite particles revealed a different picture all together – figure 4.7c). Investigating the sample, utilizing a scanning electron microscope (SEM), revealed the presence of iron rich exsolutions on the particle surface not present in the unroasted particles - refer to figure 4.8 and table 4.12.

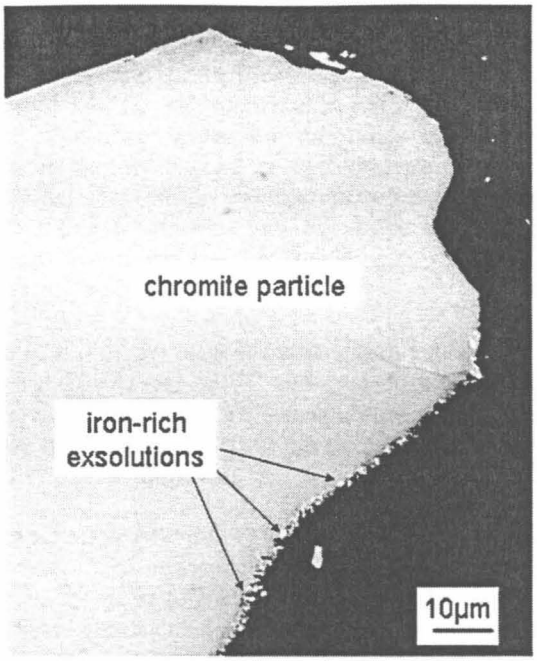

Figure 4.8: SEM micrograph (back-scattered electron image) of a UG1 chromite particle roasted at 750°C in air for 20 minutes indicating iron rich exsolutions on the particle surface.

Table 4.12: Chemical composition (EDX), in mass per cent, of the iron rich exsolution in the UG 1 chromite roasted at 750°C for 20 minutes in air

Analysis number	Element mole %					Element mass %				
	Si	Cr	Fe	Mg	Al	Si	Cr	Fe	Mg	Al
1	0.2	16.9	67.3	5.1	10.5	0.1	17.4	74.4	2.5	5.6
2	0.9	10.1	63.3	18.2	7.6	0.6	11.1	74.7	9.3	4.3
3	1.3	11.7	64	12.5	10.4	0.8	12.7	74.3	6.3	5.9
4	3	16.3	57.4	14.2	9.1	1.8	17.9	67.8	7.3	5.2
5	7.3	12	53.9	15.9	10.9	4.6	13.8	66.6	8.6	6.5
6	2.1	7.4	62.8	7.5	20.2	1.3	8.3	75	3.9	11.6
7	1.4	7.2	61.7	24.7	5	0.8	8.2	75	13.1	2.9
8	0.7	9.7	58.8	25	5.8	0.4	11.1	71.8	13.3	3.4
9	0.2	36.2	24.6	16	23	0.2	44.1	32.1	9.1	14.5
10	0	39	26.2	13.3	21.5	0	46.2	33.2	7.4	13.2
11	0	39.4	25.6	13.2	21.8	0	46.7	32.6	7.3	13.4
12	0.1	39	26.4	13.1	21.4	0.1	46.1	33.5	7.2	13.1
13	0.3	37.8	26.3	14.1	21.5	0.2	45.1	33.6	7.8	13.3
14	0.3	38.8	26.1	13.4	21.3	0.2	46	33.3	7.4	13.1
15	0	38.3	27.4	13	21.4	0	45.1	34.6	7.2	13.1
16	0.1	37.9	26.9	14	21.1	0	44.9	34.2	7.8	13
Average	**1.1**	**24.9**	**43.7**	**14.6**	**15.8**	**0.7**	**29.0**	**52.9**	**7.8**	**9.5**
Standard deviation	1.9	14.1	18.3	5.0	6.8	1.2	17.2	20.3	2.7	4.4
Minimum	0.0	7.2	24.6	5.1	5.0	0.0	8.2	32.1	2.5	2.9
Maximum	7.3	39.4	67.3	25.0	23.0	4.6	46.7	75.0	13.3	14.5

It is postulated here that these iron rich exsolutions is the cause of the increase in magnetic susceptibility observed in figure 4.6. This mechanism would be similar to that described for ilmenite by Guzman, Taylor and Giroux (1992). It would be valuable to study this mechanism further by subjecting UG 1 chromite to longer residence times (60, 120 and 180 minutes) at 750°C in air, included in the future study.

The effect of variation in temperature on magnetic susceptibility was not as strong for the chromite as for the ilmenite – represented by LSR. The different effects are shown in greater detail in figure 4.9 a) to d). As shown by figure 4.9 a) and b), the ilmenite increased significantly in magnetic susceptibility after roasting at 700°C and 750°C, and significantly more so than the chromite. This is of course favourable for magnetic separation, where the difference in magnetic susceptibility between the ilmenite and the chromite is used to separate the two minerals. Roasting at 750°C is more favourable for magnetic separation than at 700°C, yielding differences in magnetic susceptibility (between ilmenite and chromite) of factors of three and two respectively. For these two temperatures, no significant decrease in magnetic susceptibility of the ilmenite below that of the chromite was observed for the roasting times used in this study.

As illustrated by figure 9 c) and d), the magnetic susceptibility of the ilmenite increased strongly at first (for 5 minutes' roasting) at 800°C and 850°C and then decreased below that of the chromite upon further roasting. The decrease in the magnetic susceptibility of the ilmenite was due to over-roasting. Over-roasting of chromite was only observed in one case, and then it was a weak effect, namely after 40 minutes' roasting at 850°C (see figure 4.6).

The large change in the magnetic susceptibility of the ilmenite for roasting at 850°C for relatively small differences in retention times is an undesired effect: the control of the retention time in the roasting reactor would have to be very precise to ensure separation of ilmenite from chromite. This is unlikely to be practical in industrial-scale reactors. When roasting the LSR under the tested conditions, more than one control strategy could be followed:

- High temperature, short retention time e.g. at 800°C for 5-10 minutes. The risk of over-oxidation would be high and the retention time of material in a reactor should be closely controlled. Equipment suitable for this process would be a batch reactor or a plug flow reactor with a very good control system (Levenspiel 1999)
- Lower temperature, longer retention time e.g. at 750°C for 10-40 minutes or even more. Although the maximum increase in magnetic susceptibility was not reached, a larger range of retention times in the reactor would result in very similar increases in magnetic susceptibility. This strategy would therefore be very suitable for a reactor where material had a retention time distribution, e.g. a continuous stirred tank reactor (CSTR) (Levenspiel 1999).

4.2.2 Concluding interpretation

The results in figure 4.2 and figure 4.3 confirm the observations made by Nell & Den Hoed (1997) when investigating the roasting of crude ilmenite: the rate of oxidation is controlled by temperature rather than gas composition.

The results of this study clearly indicate that the hypothesis that the magnetic susceptibility of chromite remains constant during magnetising roasting of an ilmenite concentrate under the oxidising conditions as used before, is not true. A change in the magnetic susceptibility of the UG 1 chromite was observed, but it was not large and it is postulated here that the mechanism for this change is the formation of iron rich exsolutions with a higher magnetic susceptibility than the chromite matrix during oxidative roasting.

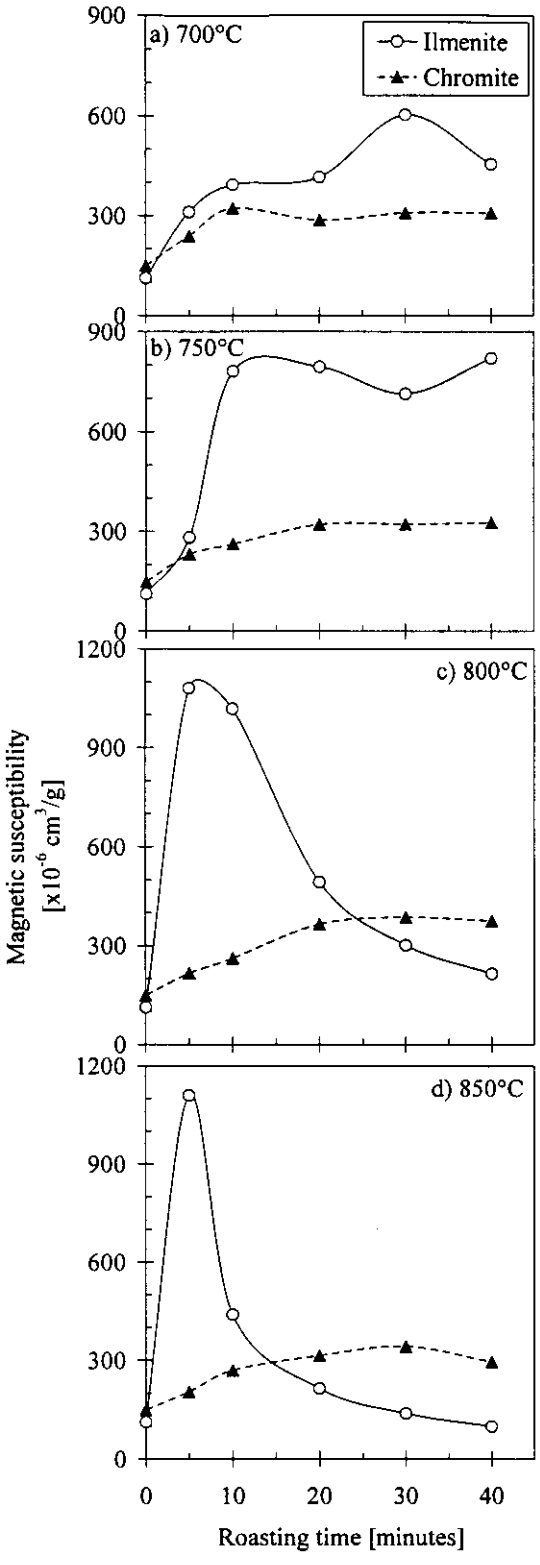

Figure 4.9: Magnetic susceptibility of LSR and UG1 chromite samples after roasting for different time intervals in air, at different temperatures: a) 700°C, b) 750°C, c) 800°C and d) 850°C.

Based on the assumptions that the bulk magnetic susceptibility of the LSR samples represents that of the ilmenite in the LSR, and the bulk magnetic susceptibility of UG1 chromite that of the of chromite in the LSR, the results also served to confirm that following observations regarding the conditions required for maximal separation between ilmenite and chromite:

The LSR with a high chromite content should be roasted under oxidising conditions, in a reactor with a well-defined retention time distribution (i.e. a fluidized bed reactor), at a roasting temperature of 750°C (rather than the higher temperature ranges of 800°C and 850°C).

4.3 Fractionation of crude ilmenite, LSR and UG 1 chromite before roasting

4.3.1 Presentation and discussion of results

In figure 4.10a) and 4.11a) separability curves are presented for the TiO_2 and Cr_2O_3 content of unroasted samples of crude ilmenite and LSR respectively.

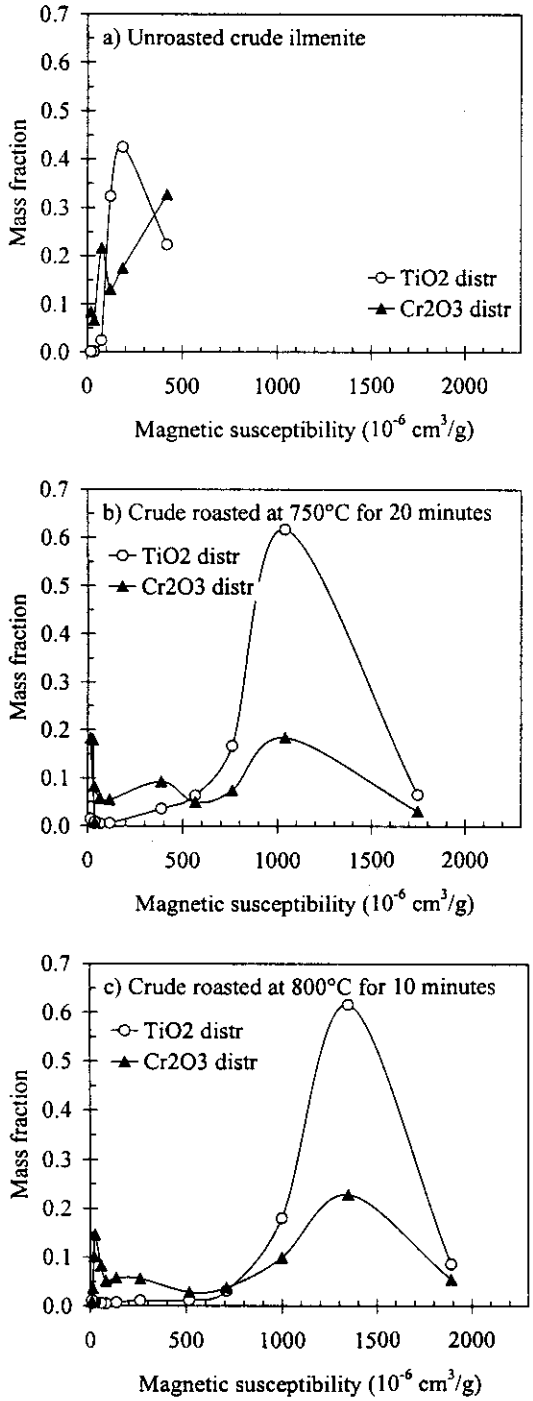

Figure 4.10: Separability curves indicating the TiO_2 and Cr_2O_3 distributions in a) unroasted crude ilmenite; b) crude ilmenite roasted at 750°C for 20 minutes in air and c) crude ilmenite roasted at 800°C for 10 minutes in air.

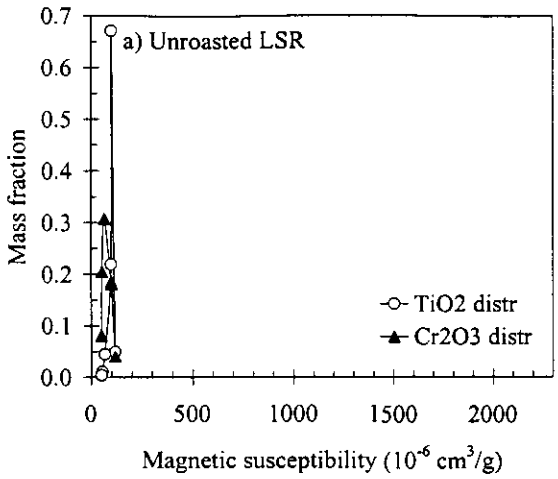

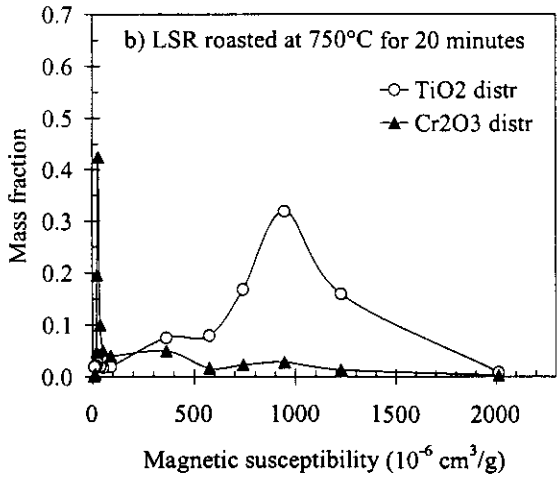

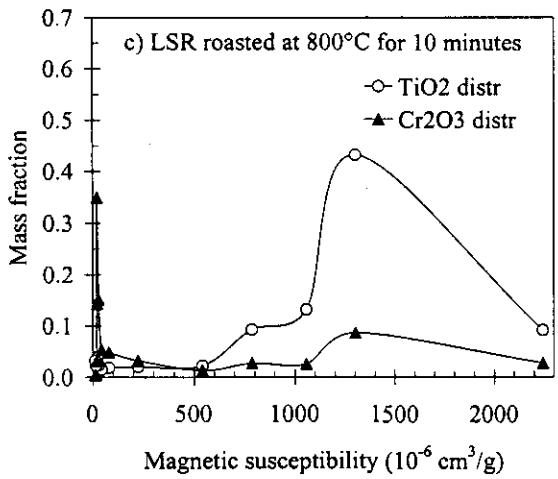

Figure 4.11: Separability curves indicating the TiO_2 and Cr_2O_3 distributions in a) unroasted LSR; b) roasted at 750°C for 20 minutes in air and c) LSR roasted at 800°C for 10 minutes in air. The units of measurement for magnetic susceptibility are cm^3/g.

The assumption was made that TiO_2 in the chemical analysis of each fraction represented ilmenite only and Cr_2O_3 chromite. This was not necessarily true as TiO_2 could represent ilmenite, rutile or pseudorutile. The fractionation data utilized to construct these curves are presented in table 4.13 for unroasted LSR and table 4.14 for crude ilmenite.

Table 4.13: Fractionation results for unroasted LSR – field strength reported in Gauss; mass fraction as per cent; magnetic susceptibility reported as $*10^{-6}$ cm^3/g; and chemical components as mass per cent

Field strength	Mass fraction	Magnetic susceptibility	TiO_2	Cr_2O_3
1375	10.7	117	19	0.20
2150	60.6	100	45	0.16
2735	19.5	99	46	0.51
3450	5.6	66	33	2.96
4050	1.8	54	25	6.14
4650	0.7	50	25	6.20

Table 4.14: Fractionation results for unroasted crude ilmenite – field strength reported in Gauss; mass fraction as per cent; magnetic susceptibility reported as $*10^{-6}$ cm^3/g; and chemical components as mass per cent

Field Strength	Mass fraction	Magnetic susceptibility	TiO_2	Cr_2O_3
1375	23.2	418	46	0.25
2150	42.4	184	47	0.07
2735	30.7	120	50	0.08
3450	3.0	74	40	1.30
4050	0.3	36	23	4.22
4650	0.3	19	21	5.50

The TiO_2 and Cr_2O_3 distributions of unroasted crude ilmenite in figure 4.10a) did not have a fraction of the 'high susceptible rejects' as described by Beukes and Van Niekerk (1999). This implies that the 'crude ilmenite' roasted in the fractionation exercise was more of an 'HSR-stripped crude ilmenite'. The HSR was most probably removed by the LIMS operation during pilot plant trials. The bimodal populations observed by Nell and Den Hoed (1997) for Cr_2O_3 were absent from these samples. In the unroasted LSR sample the TiO_2 was concentrated in a single population to the higher magnetic susceptible side. Cr_2O_3 was distributed over a larger range of magnetic susceptibility (perhaps reflecting the range of compositions shown in figure 4.1).

Representing the same set of data in a different manner recovery data sets were developed for both TiO_2 and Cr_2O_3 in unroasted crude ilmenite and unroasted LSR. The data for Cr_2O_3 are plotted in figure 4.12a) and figure 4.13a). Recall that the Cr_2O_3 content must be less than 0.1 per cent to meet the specification.

In figure 4.14 separability curves for ilmenite (represented by LSR), chromite in LSR and UG1 chromite are presented. The data used for these curves are reported in table 4.13 and table 4.15. In these separability curves the mass fraction is plotted as a function of the applied magnetic field strength and not as the inverse of magnetic susceptibility as in previous separability curves. Both the ilmenite curve and the UG 1 chromite curve have tight, single distributions while the chromite in the LSR has a wider distribution, but with a peak at the same field strength as the UG 1 chromite.

Table 4.15: Fractionation results for unroasted UG 1 chromite – field strength reported in Gauss and mass fraction as per cent

Field Strength	Mass fraction
1375	0.0
2150	0.1
2735	3.4
3450	96.1
4050	0.4

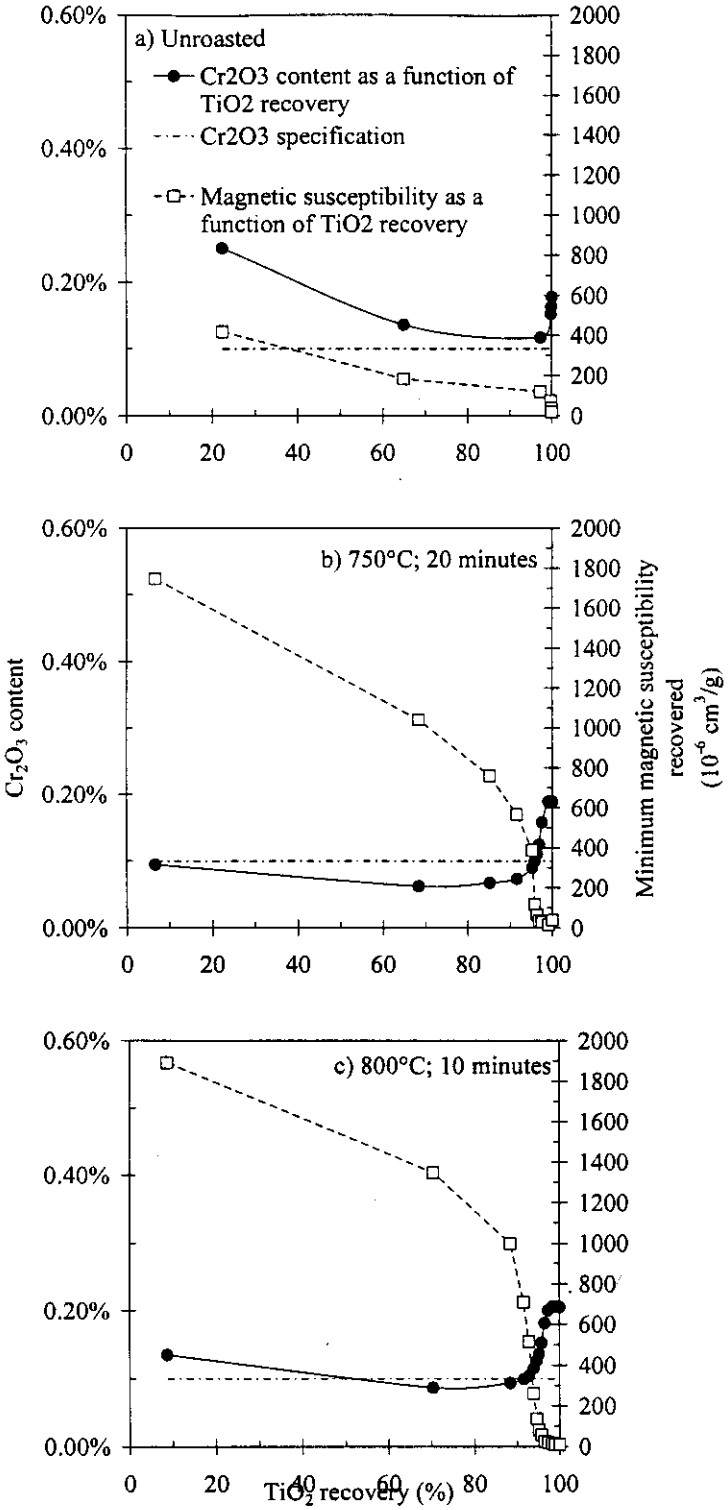

Figure 4.12: Recovery curves of crude ilmenite indication the Cr_2O_3 distribution in a) unroasted crude ilmenite; b) crude ilmenite at 750°C for 20 minutes in air and c) crude ilmenite roasted at 800°C for 10 minutes in air.

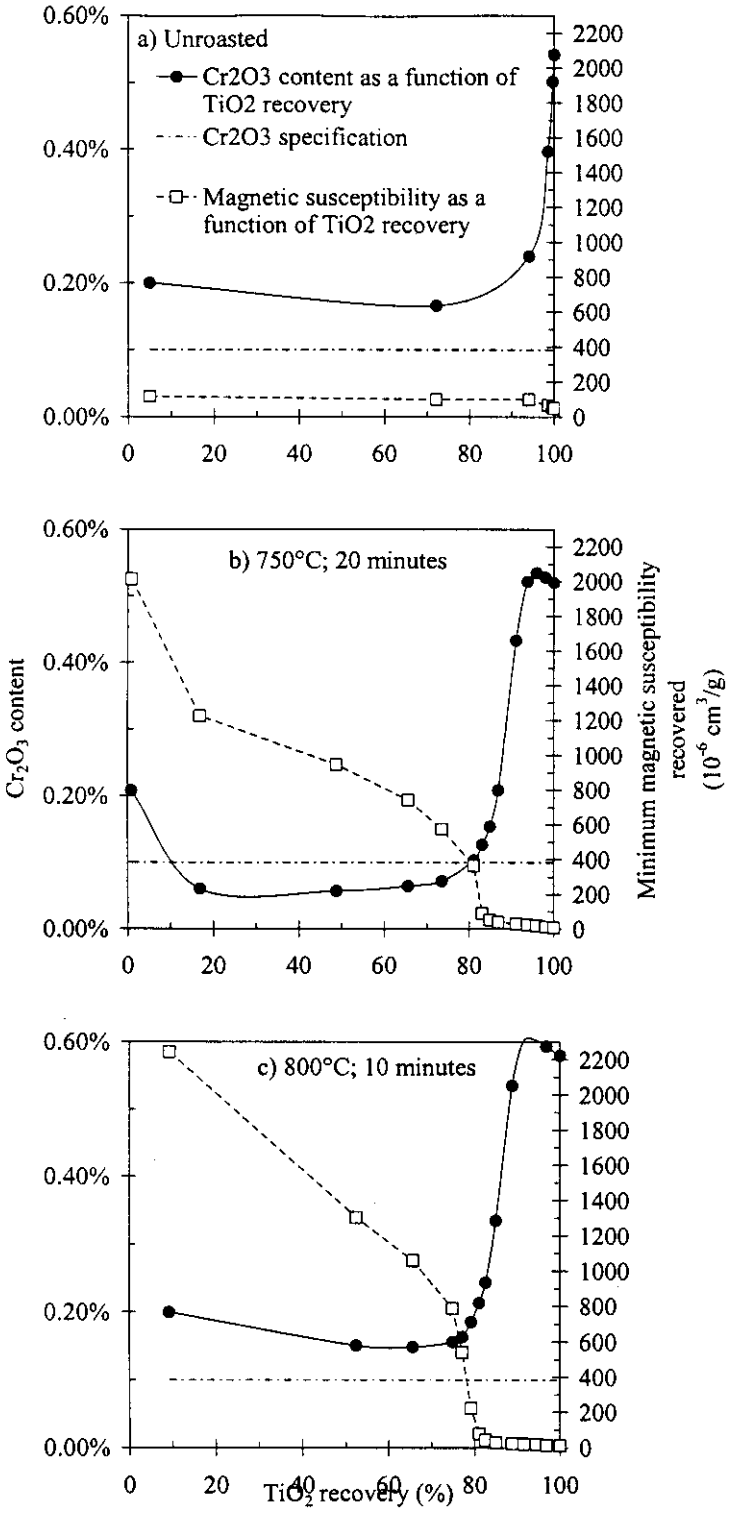

Figure 4.13: Recovery curves of LSR indication the Cr_2O_3 distribution in a) unroasted LSR, b) LSR roasted at 750°C for 20 minutes in air and c) LSR roasted at 800°C for 10 minutes in air.

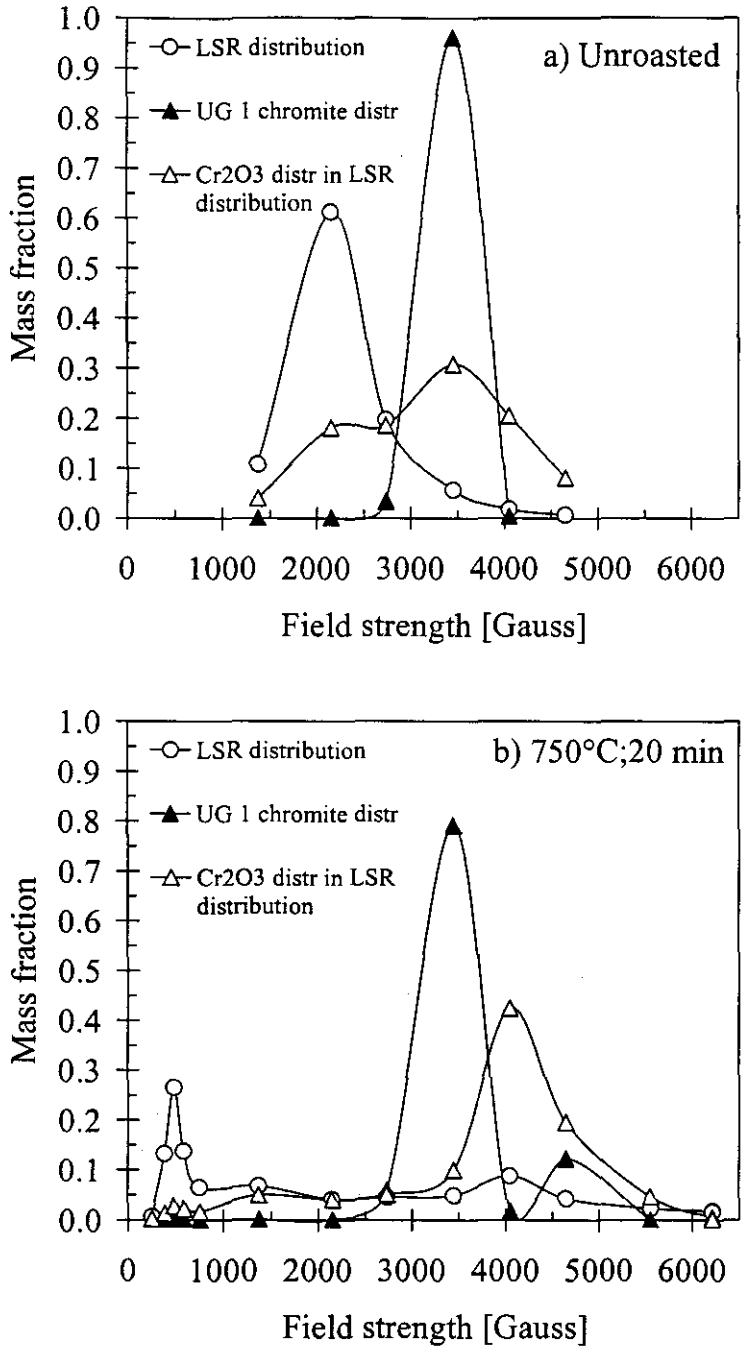

Figure 4.14: Separability curves indicating the mass distribution of a) unroasted LSR, the chromite in unroasted LSR and unroasted UG1 chromite, and b) LSR, chromite in LSR and UG 1 chromite roasted at 750°C for 20 minutes, when fractionated at various field strengths.

4.3.2 Concluding interpretation

From figure 4.12a) and 4.13a) it is concluded that without roasting a product with acceptably low Cr_2O_3 cannot be produced from either crude ilmenite or LSR. The results in figure 4.14 indicate that the UG 1 chromite represented at least part of the chromite in the LSR.

4.4 Fractionation of crude ilmenite, LSR and UG 1 chromite after roasting

4.4.1 Presentation and discussion of results

After roasting crude ilmenite at 750°C for 20 minutes in air the TiO_2 distribution was concentrated in a single population and the Cr_2O_3 distribution was bimodal (see figure 4.10b). Roasting resulted in an increase in the magnetic susceptibility, in the order of $856x10^{-6}$ cm^3/g, for the peak in the TiO_2 distribution. The values obtained at the bimodal Cr_2O_3 peaks were $622x10^{-6}$ cm^3/g and $39x10^{-6}$ cm^3/g respectively. The recovery curve in figure 4.12b) indicates that the percentage Cr_2O_3 in the ilmenite was 0.1 per cent or less at titanium recoveries ranging from 7 to 95 per cent. The maximum recovery would be obtained by removing material with a magnetic susceptibility of less than about 400 x 10^{-6} cm^3/g.

After roasting the crude ilmenite at 800°C for 10 minutes in air (figure 4.10c) the TiO_2 distribution was concentrated in a single population and the Cr_2O_3 distribution was bimodal as also observed by Nell & Den Hoed (1997). Roasting resulted in a significant increase in the magnetic susceptibility, in the order of $1163x10^{-6}$ cm^3/g, for the peak in the TiO_2 distribution. A significant increase in magnetic susceptibility of Cr_2O_3, similar to the TiO_2 peak i.e. in the order of $1163x10^{-6}$ cm^3/g, was observed for the peak in the Cr_2O_3 distribution to the high susceptible side and a slight decrease of $159x10^{-6}$ cm^3/g for that to the low susceptible side. In figure 4.12c) the per cent Cr_2O_3 in ilmenite recovered from HSR stripped crude ilmenite reached values of less than 0.1 per cent at titanium recoveries ranging from 55 per cent to 95 per cent. The maximum recovery would be obtained by removing material with a magnetic susceptibility of less than about 1000 x 10^{-6} cm^3/g.

The fractionation results for LSR roasted at 750°C for 20 minutes in air in figure 4.11b) were very interesting: both the TiO_2 and the Cr_2O_3 distributions concentrated in single populations. The peak magnetic susceptibility of the TiO_2 increased with $845x10^{-6}$ cm^3/g and that of the Cr_2O_3 decreased with $37x10^{-6}$ cm^3/g. The result of this 'ideal' magnetic behaviour of the chromite and the ilmenite was the production of ilmenite with 0.1 per cent Cr_2O_3 or less at titanium recoveries of 10-80 per cent (figure 4.13b)! The maximum recovery would be obtained by removing material with a magnetic susceptibility of less than about 400 x 10^{-6} cm^3/g.

After roasting LSR at 800°C for 10 minutes in air (figure 4.11c) the TiO_2 distribution was concentrated in a single population, but spread over a wider range of susceptibilities than in the unroasted sample. The Cr_2O_3 distribution was bimodal. Roasting resulted in a significant increase in the magnetic susceptibility, in the order of $1200x10^{-6}$ cm^3/g, for the peak in the TiO_2 distribution. A slight decrease in magnetic susceptibility, in the order or $44x10^{-6}$ cm^3/g, was observed for the peak in the Cr_2O_3 distribution. In figure 4.13c) the per cent Cr_2O_3 in the recovered sample never reached the specification of <0.1 per cent.

The bimodality of the Cr_2O_3 distribution when roasting LSR at 800°C for 10 minutes in air could be due to:

- The low concentration of Cr_2O_3 in the fractions (i.e. an analytical error);
- Roasting under the specific conditions also increased the magnetic susceptibility of the chromite in the LSR fraction; or
- Different chromites in the LSR (based on chemical composition as in figure 4.1) reacts differently under the roasting conditions.

If either or the last two situations were the case it would be a problem as one would not be able to beneficiate ilmenite from chromite. The recovery curves illustrated the problem of ilmenite beneficiation from chromite in LSR more clearly. This observation gave rise to the part of the test program that tested the hypothesis that the magnetic susceptibility of the chromite did not change during roasting.

In figure 4.14b) separability curves for ilmenite (represented by LSR), chromite in LSR and chromite (represented by UG1 chromite) roasted at 750°C for 20 minutes were constructed. The data used for these curves are listed in table 4.14 and table 4.16. In these separability curves the mass fraction is plotted as a function of the applied magnetic field strength and not as the magnetic susceptibility as in previous separability curves. The UG 1 chromite curve had a bimodal distribution indicating a slight decrease in the magnetic susceptibility of some of the chromite after roasting, but also the presence of a slightly larger fraction at the field strength just lower than the peak value. Presumably the size of the

intervals used in these measurements was too large to detect the changes which resulted in the slight increase in bulk magnetic susceptibility shown in Figure 4.6. Although the chromite in the LSR had a tighter distribution than in the unroasted condition the average magnetic susceptibility of the chromite also appeared to decrease after roasting.

Table 4.16: Fractionation results for UG 1 chromite roasted at 750°C for 20 minutes – field strength reported in Gauss and mass fraction as per cent

Field Strength	Mass fraction
250	0.3
384	0.2
481	0.1
584	0.1
751	0.1
1375	0.1
2150	0.1
2735	5.8
3450	79.1
4050	1.7
4650	12.3
5550	0.0

4.4.2 Concluding interpretation

The results in figures 4.10b) and figure 4.11c) indicated that even if roasting decreased the bulk magnetic susceptibility of chromite in a crude ilmenite concentrate, it increased the magnetic susceptibility of some of the chromite particles, just as it did for ilmenite. In roasted, HSR stripped, crude ilmenite there was sufficient magnetically enhanced ilmenite to dilute the effect of the increase in magnetic susceptibility of chromite. In roasted LSR the ilmenite was insufficient to dilute the chromite. The effect was seen in figure 4.12c) and figure 4.13c) where ilmenite, with less than 0.1 per cent Cr_2O_3 could be recovered from crude ilmenite but not from LSR. It was possible to produce a suitable product from LSR, though, (figure 4.13b) within the range of conditions published for crude ilmenite in literature. The hypothesis that it would be possible to produce an ilmenite product suitable for ilmenite smelting by subjecting LSR to roasting and subsequent magnetic separation, at the roasting conditions published for crude ilmenite by Nell and Den Hoed (1997) or Bergeron and Prest (1974) hence survived the experimental tests applied here. Oxidising roasting did affect the magnetic susceptibility of chromite.

In short: The results from the test program were presented, discussed and interpreted. I started the discussion with the results from the feed characterization tests: the chemical analyses, the mineralogical analyses and the magnetic susceptibility. Then the results of the determination of the optimum roast conditions followed. I ended the chapter with the results from the fractionation at optimal roast conditions that was the separability curves for the unroasted and roasted material. In chapter 5 the study will be concluded and recommendations made regarding implementation and future studies.

4.5 Appendix 2: Method used to calculate the composition of the chromite from elemental EDX or WDS analysis.

4.5.1 Assumptions

1. All the chromium is trivalent i.e. Cr^{3+};
2. The chromium spinel is stoichiometric i.e. M_3O_4;
3. In natural magnesiochromites Fe^{2+} replaces Mg^{2+} to some extent and Al^{3+} and Fe^{3+} replace Cr^{3+} to some extent;
4. The composition of natural magnesiochromites could be simplified to containing MgO, FeO, Fe_2O_3, Cr_2O_3 and Al_2O_3 only.

4.5.2 Calculations

4.5.2.1 Calculation 1: The Fe^{2+} and Fe^{3+} content of the mineral

The data that would be available for the calculation of the Fe^{2+} and Fe^{3+} content of a stoichiometric chromite spinel is as in table 4.17.

Table 4.17: Data available when calculating the Fe^{2+} and Fe^{3+} content of the chromium spinel from elemental WDS and EDX analyses

Element	Assumed valence state	Molar mass	Mole per cent
O	2-	16.0	As received
Mg	2+	24.3	As received
Fe_{total}	2+ and 3+	55.9	As received
Al	3+	27.0	As received
Cr	3+	52.0	As received

The Fe^{2+} content is calculated according to equation 4.2 and the Fe^{3+} content according to equation 4.3 where $^{m}/_{o}$ means mole per cent.

Equation 4.2: Calculation of the Fe^{2+} content of a stoichiometric chromite spinel

$$n^{Fe2+} = \tfrac{1}{3}(n^{Cr3+} + n^{FeTotal} + n^{Al3+} - 2\,n^{Mg2+})$$

Equation 4.3: Calculation of the Fe^{3+} content of a stoichiometric chromite spinel

$$^{m}/_{o}Fe^{3+} = {}^{m}/_{o}Fe_{total} - {}^{m}/_{o}Fe^{2+}$$

Equation 4.2 was derived as follows: the mole ratio of M^{2+}:O:M^{3+}:O in stoichiometric spinel (M_3O_4 or $M^{2+}O.M^{3+}{}_2O_3$) is 1:1:2:3. This means that the spinel would contain half a mole of cation in the trivalent state for every mole of cation in the divalent state as in equation 4.4 where *n* is the mole fraction of a cation:

Equation 4.4: Balance of divalent and trivalent cations in a stoichiometric spinel

$$n^{2+} = \tfrac{1}{2}n^{3+}$$

The divalent cations in the magnesiochromites are Fe^{2+} and Mg^{2+} and the trivalent cations Al^{3+}; Fe^{3+} and Cr^{3+}. Incorporating this knowledge in equation 4 leads to equation 4.5:

Equation 4.5: Incorporating the divalent and trivalent cations for a magnesiochromite in equation 4.4

$$(n^{Fe2+} + n^{Mg2+}) = \tfrac{1}{2}(n^{Cr3+} + n^{Fe3+} + n^{Al3+})$$

From table 4.17 the results reported in the WDS or EDX analyses are for the total Fe content of the mineral. In the mineral itself the Fe are in both the divalent or trivalent states. This leads to the mass balance in equation 4.6:

Equation 4.6: Mass balance of iron in the magnesiochromite spinel

$$n^{FeTotal} = n^{Fe3+} + n^{Fe2+}$$

or

$$n^{Fe3+} = n^{FeTotal} - n^{Fe2+}$$

Equation 4.2 is then derived from equation 4.5 and equation 4.6 as in the series of equations in equation 4.7:

Equation 4.7: Derivation of equation 4.2 from equation 4.5 and equation 4.6

$$\begin{aligned}
(n^{Fe2+} + n^{Mg2+}) &= \tfrac{1}{2}(n^{Cr3+} + n^{FeTotal} - n^{Fe2+} + n^{Al3+}) \\
2\ (n^{Fe2+} + n^{Mg2+}) &= (n^{Cr3+} + n^{FeTotal} - n^{Fe2+} + n^{Al3+}) \\
2\,n^{Fe2+} + 2\,n^{Mg2+} + n^{Fe2+} &= n^{Cr3+} + n^{FeTotal} + n^{Al3+} \\
3\,n^{Fe2+} &= n^{Cr3+} + n^{FeTotal} + n^{Al3+} - 2\,n^{Mg2+} \\
n^{Fe2+} &= \tfrac{1}{3}(n^{Cr3+} + n^{FeTotal} + n^{Al3+} - 2\,n^{Mg2+})
\end{aligned}$$

Therefore if the results of equation 4.3 are negative (negative Fe^{3+} content) it would mean that iron are only present in the divalent state in the magnesiochromite spinel.

4.5.2.2 Calculation 2: The composition of the mineral

Once the molar per cent Fe^{2+} and Fe^{3+} of the mineral has been determined the composition of the mineral can be derived by firstly calculation the mass and then the mass per cent of each component in the mineral. The equations for these calculations are given in table 4.18 – note the difference in the mass calculations for components in the divalent and trivalent state. For these calculations the information in table as well as the results of equation 4.2 and equation 4.3 is utilized.

Table 4.18: Equations used to calculate the mass per cent of the components in the chromium spinel from elemental WDS and EDX analyses where $^{m}/_{o}$ means mole per cent and $^{w}/_{o}$ mass per cent.

Component	Mass calculations	Mass per cent calculations
MgO	$MgO_{mass} = {}^{m}/_{o}\ Mg^{2+} \times MgO_{molar\ mass}$	$^{w}/_{o}\ MgO = MgO_{mass} / total_{mass} \times 100$
FeO	$FeO_{mass} = {}^{m}/_{o}\ Fe^{2+} \times FeO_{molar\ mass}$	$^{w}/_{o}\ FeO = FeO_{mass} / total_{mass} \times 100$
Fe_2O_3	$Fe_2O_{3\ mass} = {}^{m}/_{o}\ Fe^{3+} \times ½(Fe_2O_{3\ molar\ mass})$	$^{w}/_{o}\ Fe_2O_3 = Fe_2O_{3\ mass} / total_{mass} \times 100$
Cr_2O_3	$Cr_2O_{3\ mass} = {}^{m}/_{o}\ Cr^{3+} \times ½(Cr_2O_{3\ molar\ mass})$	$^{w}/_{o}\ Cr_2O_3 = Cr_2O_{3\ mass} / total_{mass} \times 100$
Al_2O_3	$Al_2O_{3\ mass} = {}^{m}/_{o}\ Al^{3+} \times ½(Al_2O_{3\ molar\ mass})$	$^{w}/_{o}\ Al_2O_3 = Al_2O_{3\ mass} / total_{mass} \times 100$
Total	$Total_{mass} = MgO_{mass} + FeO_{mass} + Fe_2O_{3\ mass} + Cr_2O_{3\ mass} + Al_2O_{3\ mass}$	

4.5.2.3 Calculation 3: The normalized elemental composition of the mineral

For ease of interpretation and comparison of results the elemental results from the EDX and WDS analysis (in mole per cent) are normalized by dividing the mole per cent of a specific element by the totalized mole per cent of the elements in the analysis. As an example the chrome content of the magnesiochromite is normalized in equation 4.8:

Equation 4.8: Example of normalized elemental results

$$^{m}/_{o}\ Cr_{normalised} = {}^{m}/_{o}\ Cr / ({}^{m}/_{o}\ Mg + {}^{m}/_{o}\ Fe_{total} + {}^{m}/_{o}\ Al + {}^{m}/_{o}\ Cr) \times 100$$